

Tau-positive nuclear indentations in P301S tauopathy mice

Marta Fernández-Nogales^{1,2*}, María Santos-Galindo^{1,2*}, Jesús Merchán-Rubira^{1,2*}, Jeroen Hoozemans³, Alberto Rábano^{2,4}, Isidro Ferrer^{2,5}, Jesús Avila^{1,2}, Félix Hernández^{1,2} and José J. Lucas^{1,2}

¹Center for Molecular Biology “Severo Ochoa” (CBMSO) CSIC/UAM, 28049 Madrid, Spain

²Networking Research Center on Neurodegenerative Diseases (CIBERNED). Instituto de Salud Carlos III, Spain.

³Department of Pathology, VU University Medical Center, Neuroscience Campus Amsterdam, 1007 MB Amsterdam, The Netherlands.

⁴Departamento de Neuropatología y Banco de Tejidos, Fundación CIEN, Madrid, Spain.

⁵Institute of Neuropathology; IDIBELL-University Hospital Bellvitge; University of Barcelona; Hospitalet de Llobregat; Barcelona 08908, Spain.

*These authors contributed equally

Corresponding author: José J. Lucas

Centro de Biología Molecular “Severo Ochoa” (CSIC/UAM)
C/ Nicolás Cabrera,1
Campus UAM de Cantoblanco
28049 Madrid. Spain
Tel. +34 91 196 4552/ +34 91 196 4582
e-mail: jjlucas@cbm.csic.es
<http://www.cbm.uam.es/lineas/lucasgroup.htm>

Keywords: Tau, TNR (tau nuclear rod), nuclear indentations, TNI (tau-immunopositive nuclear indentation), tauopathy

This article has been accepted for publication and undergone full peer review but has not been through the copyediting, typesetting, pagination and proofreading process which may lead to differences between this version and the Version of Record. Please cite this article as an ‘Accepted Article’, doi: 10.1111/bpa.12407

ABSTRACT

Increased incidence of neuronal nuclear indentations is a well-known feature of the striatum of Huntington's disease (HD) brains and, in Alzheimer's disease (AD), neuronal nuclear indentations have recently been reported to correlate with neurotoxicity due to improper cytoskeletal/nucleoskeletal coupling. Initial detection of rod-shaped tau immunostaining in nuclei of cortical and striatal neurons of HD brains and in hippocampal neurons of early Braak stage AD led us to coin the term "tau nuclear rods (TNRs)". Although TNRs traverse nuclear space, they in fact occupy narrow cytoplasmic extensions that fill indentations of the nuclear envelope and we will here refer to this histological hallmark as Tau-immunopositive nuclear indentations (TNIs). We reasoned that TNI formation is likely secondary to tau alterations as TNI detection in HD correlates with an increase in total tau, particularly of the isoforms with four tubulin binding repeats (4R-tau). Here we analyze transgenic mice that overexpress human 4R-tau with a frontotemporal lobar degeneration-tau point mutation (P301S mice) to explore whether tau alteration is sufficient for TNI formation. Immunohistochemistry with various tau antibodies, immunoelectron microscopy and double tau-immunofluorescence/DAPI-nuclear counterstaining confirmed that excess 4R-tau in P301S mice is sufficient for the detection of abundant TNIs that fill nuclear indentations. Interestingly, this does not correlate with an increase in the number of nuclear indentations, thus suggesting that excess total tau or an isoform imbalance in favor of 4R-tau facilitates tau detection inside preexisting nuclear indentations but does not induce formation of the latter. In summary, here we demonstrate that tau alteration is sufficient for TNI detection and our results suggest that the neuropathological finding of TNIs becomes a possible indicator of increased total tau and/or increased 4R/3R-tau ratio in the affected neurons apart from being an efficient way to monitor pathology-associated nuclear indentations.

INTRODUCTION

The presence of rod shaped nuclear structures in neurons in normal and pathological states is known for more than a century (7, 8, 19, 22). These include the rodlets of Roncoroni or intranuclear rodlets among others and there have been many efforts to identify their constituent proteins (20, 30). Such rodlets have been associated with various neurodegenerative diseases like frontotemporal lobar degeneration (FTLD) (29), Alzheimer's disease (AD) (32) or Parkinson's Disease (17).

On the other hand, rod shaped indentations of the nuclear envelope are also frequent in neurons (15, 24), their incidence has been reported to change as a consequence of the synaptic activity of the neurons (28) and increased incidence has been known for decades in striatum of Huntington's disease (HD) brain and more recently also in related CAG triplet repeat disorders patients (4, 23, 25) and cell and mouse models (10, 11, 34). Interestingly, neuronal nuclear indentations have also recently been reported in AD and correlate with the improper cytoskeletal/nucleoskeletal coupling that has been suggested as a novel mediator of neurotoxicity in tauopathies (13).

Tauopathies are a group of neurodegenerative diseases characterized by altered metabolism and deposition of the neuronal microtubule associated protein tau (MAPT) (2, 18). The discovery of mutations in the *MAPT* gene as causative of familial FTLD-tau evidenced that tau alteration is sufficient to cause neurodegenerative disease (16). Apart from point mutations, FTLD-tau can also be caused by silent and intronic mutations that affect the alternative splicing event that generates tau isoforms with either three or four tubulin binding repeats (3R- and 4R-tau), thus demonstrating that an imbalance in the 3R/4R-tau ratio is pathological *per se*.

Neuronal tau nuclear rods (TNRs) were recently described as nuclear rodlet-shaped tau immunostainings in neurons of cortex and striatum of HD brains (12, 27 and reviewed in 14) and in hippocampus of early Braak stage AD brains (12). TNRs appear to traverse the nuclear space (12, 27). However, immunoelectron microscopy or confocal analysis of tau immunofluorescence with a fluorescent nuclear counterstaining revealed that TNRs in brains of HD patients in fact occupy narrow cytoplasmic extensions that fill infoldings of the nuclear envelope (12) and we will here refer to this histological hallmark as Tau-immunopositive nuclear indentations (TNIs). TNI formation is likely secondary to tau alterations as TNI detection in HD correlates with an increase in total tau, particularly of the isoforms with four tubulin binding repeats (4R-tau). However, it cannot be ascertained that the formation of the TNIs is a direct consequence of tau alteration.

Here we analyze transgenic mice that overexpress human 4R-tau with a FTL tau point mutation (P301S mice) to explore whether tau alteration is sufficient for the detection of TNIs. Immunohistochemistry with various tau antibodies, immunoelectron microscopy and double tau-immunofluorescence/DAPI-nuclear counterstaining confirmed that P301S 4R-tau overexpression in tauopathy mice is sufficient for the detection of abundant TNIs.

MATERIALS AND METHODS

Transgenic mice

P301S mice transgenic for the human tau gene in B6C3F1 background (33) were used. This mouse model carries a mutant (P301S) human *MAPT* gene encoding T34-tau isoform (1N4R); it is driven by the mouse prion-protein promoter (*Prnp*) on a B6C3H/F1 genetic background. A group of mice was analysed at the age of 20 weeks at which P301S mice show only learning deficits and another at the age of 36 weeks at which they also show motor deficits (33). A total of 6 mice at the age of 20 weeks (n=3 for WT, n=3 for P301S) and a total of 15 mice at the age of 36 weeks (n=6 for WT, n=9 for P301S) were analyzed. Tau KO mice (9) were also used in this study to demonstrate specificity of immunostaining with different anti-tau antibodies.

All mice were housed at the Centro de Biología Molecular “Severo Ochoa” animal facility. Mice were housed four per cage with food and water available *ad libitum* and maintained in a temperature-controlled environment on a 12/12 h light-dark cycle with light onset at 07:00 h. Animal housing and maintenance protocols followed the guidelines of Council of Europe Convention ETS123, recently revised as indicated in the Directive 86/609/EEC. Animal experiments were performed under protocols (P15/P16/P18/P22) approved by the Centro de Biología Molecular Severo Ochoa Institutional Animal Care and Utilization Committee (Comité de Ética de Experimentación Animal del CBM, CEEA-CBM, Madrid, Spain).

Human brain samples from HD subjects

Brain specimens used in this study from frontal cortex and striatum of two HD subjects, were provided by the Neurological Tissue Bank of the IDIBAPS Biobank (Barcelona, Spain). Written informed consent for brain removal after death for diagnostic and research purposes was obtained from brain donors and/or next of kin. Procedures, information and consent forms

have been approved by the Bioethics Subcommittee of Centro Superior de Investigaciones Científicas (Madrid, Spain). The postmortem delay in tissue processing (PMI) was 5:00 and 5:30 h. The neuropathological examination of these HD cases revealed a diagnosis of HD grade 3 following the criteria of Vonsattel (26).

Western Blot

Mouse brains were quickly dissected on an ice-cold plate. Extracts were prepared by homogenizing the brain areas in ice-cold extraction buffer, consisting of 20 mM HEPES pH 7.4, 100 mM NaCl, 20 mM NaF, 1% Triton X-100, 1 mM sodium orthovanadate, 1 μ M okadaic acid, 5 mM sodium pyrophosphate, 30 mM β -glycerophosphate, 5 mM EDTA, and protease inhibitors (2 mM PMSF, 10 μ g/ml aprotinin, 10 μ g/ml leupeptin and 10 μ g/ml pepstatin), and centrifuging at 15000 g for 15 min at 4 °C. The resulting supernatant was collected, and protein content determined by Bradford assay. Fifteen micrograms of total protein were electrophoresed on 10% SDS-polyacrylamide gel, transferred to a nitrocellulose membrane and blocked in TBS-T (150 mM NaCl, 20 mM Tris-HCl, pH 7.5, 0.05% Tween 20) supplemented with 5% non-fat dry milk or 5% BSA depending on the antibody used. Employed antibodies were anti-tau Tau5 (577801 from Calbiochem) and anti- β -actin clone AC-74 (A5316 from Sigma-Aldrich). The membranes were incubated with the primary antibody overnight at 4°C in TBS-T supplemented with 5% non-fat dry milk, washed in TBS-T, incubated with secondary HRP-conjugated anti-mouse IgG (P0447 from DAKO Cytomation) and developed using the ECL detection kit (Perkin Elmer).

Immunohistochemistry and immunofluorescence

For human samples, formalin fixed (4%, at least 3 weeks) paraffin embedded tissue from cortex and striatum were used. Sections (5 μ m thick) were mounted on superfrost-plus tissue slides (Menzel-Gläser) and deparaffinized.

All 20 week-old mice (n=3 for WT, n=3 for P301S) and 26 week-old mice Tau KO (n=2) were sacrificed using CO₂. Brains were immediately removed and dissected on an ice-cold plate and left hemispheres, processed for histology, were placed in 4% paraformaldehyde in Sorensen's phosphate buffer overnight and then immersed in 30% sucrose in PBS for 72 h. Once cryoprotected, the samples were included in OCT compound (Sakura Finetek Europe), frozen and stored at -80°C until use. 30 µm sagittal sections were cut on a cryostat (Thermo Scientific), collected and stored free floating in glycol containing buffer (30% glycerol, 30% ethylene glycol in 0,02M phosphate buffer) at -20°C.

All 36 week-old mice (n=6 for WT, n=9 for P301S) were sacrificed by intracardial perfusion under deep pentobarbital anesthesia (intraperitoneal injection) with 50 ml of 0.9% saline, followed by 50 ml of 4% paraformaldehyde in phosphate buffer. Their brains were immediately extracted and fixed overnight in the same fixative. Sagittal 50-µm-thick sections were obtained on a Leica VT1000S vibratome.

For immunohistochemistry, sections were immersed in 0.3% H₂O₂ in PBS for 30 min to quench endogenous peroxidase activity and in the case of human samples treated with 10 mM pH 6.0 citrate buffer heated by microwave during 15 min for antigen retrieval. Subsequently, sections were blocked for 1 h in PBS containing 0.5% Fetal Bovine Serum, 0.3% Triton X-100 and 1% BSA (Sigma-Aldrich) and incubated overnight at 4°C in PBS containing 0.3% Triton X-100 and 1% BSA with the corresponding primary antibody: anti-tau HT-7 (MN1000 from Thermo Scientific), anti-tau Tau5 (577801 from Calbiochem), anti-tau Tau1 (MAB342 from Chemicon), or anti-phosphorylated tau AT8 antibody (MN1020 from Thermo Scientific). Finally, brain sections were incubated with anti-mouse secondary antibody and avidin-biotin complex using the Elite Vectastain kit (Vector Laboratories). Chromogen reactions were performed with diaminobenzidine (SIGMAFAST™ DAB, Sigma) for 10 min. Mouse sections were mounted on glass slides and coverslipped with Mowiol (Calbiochem) while human sections were

dehydrated and mounted with DePeX (Serva). Images were captured using an Olympus BX41 microscope with an Olympus camera DP-70 (Olympus Denmark A/S).

For immunofluorescence, series of sections used for quantification were set by pooling together every 8th section (thus, each series comprises 8–10 sections with each section 400 μm apart from the nearest ones). Sections were incubated overnight with primary antibody HT-7, followed by washes and overnight incubation with secondary antibody conjugated with Alexa-555 fluorophore (Invitrogen). Finally, they were counterstained for 10 minutes with DAPI (Calbiochem, Merck KGaA) and mounted using FluorSave (Calbiochem, Merck KGaA). Images were obtained under a Zeiss LSM710 confocal system coupled to the invert Axioobserver microscope with a 63x, 1.4 numerical aperture oil immersion objective using the Zen2010B sp1 software (Carl Zeiss). Images were processed using ImageJ 1.45s.

Quantification of nuclei with indentations and TNIs

For quantification, researcher was blind to genotype. As HT-7 signal is only detectable in P301S mice, we first analyzed the incidence of nuclear indentations by imaging only the DAPI signal. Then, a second analysis was performed in which both HT-7 and DAPI images were taken in order to determine the overlap between nuclear indentation and HT-7 positive TNIs.

For analysis of nuclear indentation incidence, 4 randomly selected sections of each series were analyzed per animal (n=5 for WT, n=7 for P301S). In each section, nuclear rod shaped indentations were counted in a 135 \times 135 μm field of CA1 pyramidal neurons of the hippocampus. A Z-stacking of 60 planes 0.3 μm apart from each other was covered, comprising 100–150 nuclei of pyramidal neurons. The percentage of nuclei presenting indentations was calculated.

For TNIs detection, three P301S mice and three WT mice were analyzed (one section per brain). The number of nuclei with HT-7 positive TNIs was counted in a 135 \times 135 μm field of

CA1 pyramidal neurons of the hippocampus. A Z-stacking of 18 planes 0.3 μm apart from each other was covered, comprising around 50 nuclei of pyramidal neurons per image. The percentage of nuclei presenting HT-7 positive TNIs was calculated.

Electron Microscopy

For electron microscopy, sections from P301S mice subjected to immunohistochemistry with anti-tau HT-7 antibody (MN1000 from Thermo Scientific) were processed. Briefly, sections were post-fixed in 2% OsO_4 for 1 h, dehydrated, embedded in Araldite and flat-mounted in Formvar-coated slides, using plastic cover slips. After polymerization, selected areas were photographed, trimmed, re-embedded in Araldite and resectioned at 1 μm . These semi-thin sections were rephotographed and resectioned in ultrathin sections. The ultrathin sections were observed in a Jen 2010 Joel transmission electron microscope (Peabody), without heavy metal staining to avoid confounding precipitates.

Data analysis

Statistical analysis was performed with SPSS 21.0 (SPSS® Statistic IBM®). Data are represented as means \pm SEM. The normality of the data was analyzed by Shapiro-Wilk test. For 2 group comparison, two tail t-Student's test (data with normal distribution) or Mann-Whitney U-test (data with non-normal distribution) was performed. A critical value for significance of $p < 0.05$ was used throughout the study.

RESULTS

Increased 4R-tau and detection of TNIs in cortex, striatum and hippocampus of P301S mice

To investigate if tau alteration is sufficient to induce the appearance of TNIs, we decided to analyze P301S mice. These mice express, under the control of the mouse prion promoter (MoPrP), a cDNA construct encoding the human tau (1N4R) isoform with one N-terminal insert and four tubulin binding repeats harboring the P301S FTLD-tau mutation (3) (Fig. 1A). We first confirmed by western blot the overexpression of 4R-tau in these mice, which resulted in dramatically increased total tau levels in the three analyzed areas: cortex, hippocampus and striatum of P301S mice with respect to *wild type* (WT) mice (Fig. 1B; n=3; t-Student, ** $p < 0.01$, *** $p < 0.001$).

To explore whether TNIs can be detected in the brain of P301S mice, we performed immunohistochemistry on brain sections from WT and P301S mice at two different ages: 20 weeks at which P301S mice show only learning deficits and 36 weeks at which they also show motor deficits (33) to study possible progression with age and disease phenotype. Immunostaining was performed with four different tau antibodies. On one hand, HT-7 and Tau5 antibodies that detect tau independently of its phosphorylation status and, on the other hand, Tau1 and AT8 antibodies that recognize a portion of the tau molecule only when it does not contain phosphorylated residues (Tau1) or only when phosphorylated at Ser202 and Thr205 (AT8). Out of these four antibodies, HT7 recognizes only transgenic tau as its epitope sequence (PPGQK) is not conserved in mouse (SPAQK) (21). On the contrary, the epitopes of Tau5, Tau1 and AT8 are conserved between mouse and human (21) and these antibodies detect both endogenous and transgenic tau protein.

With the three non phospho-tau antibodies, we were able to detect the presence of abundant TNIs in the three analyzed areas: cortex, hippocampus and striatum of P301S mice (Fig. 2A and C) whereas no TNIs were detected in WT mice and no tau signal was found in tau KO mice (Fig. 2B). Interestingly, with the phospho-tau antibody (AT-8), TNIs were observed only in cortex of P301S mice and they were less abundant (Fig. 2C). Older mice showed slightly higher TNI incidence and, interestingly, wider and more complex TNIs were found in these older mice particularly with the Tau1 antibody that recognizes only unphosphorylated tau. With all antibodies and most remarkably with Tau1, the TNIs observed in P301S mice look very similar to those previously reported in cortex and striatum of HD patients (12), as evidenced by immunohistochemistry with the HT-7 antibody on HD samples (Fig. 2D).

To verify that these so called TNIs in P301S mice really fill nuclear indentations as previously shown for the rod shaped immunostaining reported in HD brains, we performed immunoelectron microscopy. P301S brain sections were subjected to DAB-immunohistochemistry with the HT-7 antibody. Examples of stained cortical neurons are shown in figure 3 depicting frequent indentations of the nuclear envelope with tau-immunoreactivity evidenced by the presence of DAB precipitates inside the invagination. These are very similar to the neuronal nuclear indentations harboring tau immunoreactivity in the brain of HD patients (12). As also shown in Fig. 3, TNIs can adopt different shapes and sizes in neurons from P301S mice.

No difference in the incidence of nuclear indentations between P301S and WT mice

We then aimed to test whether appearance of TNIs in P301S mice was simply due to excess tau entering already formed nuclear indentations or whether the tau transgene also induced increased formation of nuclear indentations. To be able to simultaneously quantify TNIs and nuclear indentations we decided to optimize a method of HT-7-immunofluorescence with DAPI

nuclear counterstaining. Confocal analysis of brain tissue from P301S mice confirmed that we were able to efficiently screen each nucleus for the presence of HT-7 immunoreactive rods and for nuclear indentations independently by analyzing stacks of images encompassing the entire depth of the stained nuclei and then explore the degree of coincidence in the merged images. HT-7 immunoreactive nuclear grooves are efficiently observed by this technique in neurons from the three analyzed areas: cortex, hippocampus and striatum of P301S mice (Fig. 4).

For quantification of the incidence of HT-7 immunoreactive rods and of nuclear indentations in both P301S and WT mice, we decided to focus on the CA1 region of the hippocampus as neuronal bodies are concentrated in a layer thus allowing quantification of a higher number of neurons per field. In good agreement with the immunohistochemistry data shown in Fig 2, immunofluorescence with HT-7 antibody did not detect TNIs in WT mice, despite the presence of nuclear indentations evidenced by DAPI nuclear counterstaining (Fig. 5A). In contrast, approximately 20% of neurons in CA1 region of the hippocampus of P301S mice show HT-7 positive TNIs of different shapes that fill most of the nuclear invaginations detected by DAPI (Fig. 5A-B). Interestingly, there was not a significant difference between incidence of nuclear indentations in WT and P301S mice. More precisely, $23 \pm 1.7\%$ of nuclei in CA1 region of WT mice presented indentations versus $21 \pm 4.4\%$ of the nuclei in CA1 region of P301S mice, thus demonstrating that the increased incidence of TNIs in P301S mice is not due to increased incidence of nuclear indentations.

DISCUSSION

The present study shows that overexpression of P301S 4R-tau in cortex, hippocampus and striatum of a tauopathy transgenic mouse model results in formation of TNIs that highly resemble the TNIs recently reported in cortical and striatal neurons of HD patients (12, 27).

These TNIs consist on an invagination of the nuclear envelope filled with tau immunoreactive material. The detection of TNIs in P301S mice does not correlate with an increase in the incidence of nuclear indentations, as the percentage of nuclei with indentations was similar between P301S and WT mice.

In AD, the most prevalent neurodegenerative disease with tau pathology, nuclear indentations have recently been reported and suggested to contribute to neurotoxicity as a consequence of improper cytoskeletal/nucleoskeletal coupling (13) and TNIs have also been observed by immunohistochemistry with tau antibodies in hippocampal neurons of patients at early Braak stage of AD (12). As mentioned, HD is also characterized by tau alterations, namely increased level of total tau and an imbalance of the 4R/3R-tau ratio in favor of the 4R- tau isoform (12, 27; reviewed in 14). Interestingly, increased incidence of nuclear indentations in striatal neurons of HD patients has been known for decades based on ultrastructural analysis (4, 23).

In view of this, we initially reasoned that TNI detection in HD and in P301S mice might likely arise from increased formation of nuclear indentations, maybe as a consequence of overstabilized microtubules due to excess 4R-tau, thus leading to microtubule bundling that in turn would push and deform the nuclear envelope. However, here we found that excess 4R-tau in P301S mice does not result in increased incidence of nuclear indentations. This suggests that TNI detection in HD neurons might simply be due to the presence inside the nuclear indentations of tau molecules above threshold for immunohistochemical detection, as a result of excess tau and/or increased 4R/3R-tau as these features are what HD patient and P301S

mouse neurons have in common. Therefore, immunohistological detection of TNIs in histopathological analysis of human brain pathologies and mouse models might become an indicator of excess total tau content or a 4R/3R-tau imbalance in the affected neurons.

In line with the latter, we do not believe that the P301S point mutation in transgenic tau molecules in P301S mice plays a significant role in the here reported detection of TNIs, as we suspect that similar incidence of TNIs would be present in the brains of transgenic mice with equivalent overexpression of 4R-*wild type* tau. Although the experiment to prove this has not been performed.

Although the incidence of nuclear indentations is similar in P301S and WT mice, it is still possible that tau entering into the nuclear indentation is microtubule-driven with tau inside the invagination acting as a MAP. In fact, immunoelectron microscopy images often show that tau-immunoreactivity adopts an ordered parallel distribution inside the indentations both in HD human tissue (12) and P301S mice. Interestingly, we have also detected MAP2 positive nuclear rods in striatum of HD and control subjects (6). Furthermore, in case that some of the structures reported in the past as intranuclear rodlets coincide with TNIs, there are reports of intranuclear rodlets being positive for class III β -tubulin in multiple human neuronal types (30) and in mouse dopaminergic neurons (17, 31).

Another mechanism for tau accumulation inside the nuclear indentation might be related to its ability to bind to cell membranes (1, 5), particularly when not phosphorylated (1). This fits well with the lower rate of TNI detection by immunohistochemistry when a phosphorylated tau antibody was used. It is possible that the indentation provides a socket for membrane bound tau accumulation and that the environment inside the invagination will not favor the presence of charged molecules such as the excess of phosphate groups.

This tauopathy mouse model-based study opens the possibility of TNIs being present also in human FTLD-Tau brains. However, we have performed a preliminary study and we were unable to find TNIs in the limited number of analyzed FTLD-Tau cases (I.Ferrer and J.J.Hoozemans unpublished observations). Maybe because FTLD-Tau brains are not characterized by an excess of essentially non-phosphorylated tau that seems to be the common related feature between human HD and mouse P301S brains. But further analysis will be required.

In summary, here we demonstrate that tau alteration in P301S mice is sufficient for the formation of TNIs. With the available data we cannot conclude whether these structures are pathogenic or innocuous. However, since TNIs are detected both in HD human brain and P301S mouse brain whose only common abnormality is increased level of tau, particularly of the 4R-tau isoform, the detection of TNIs in histopathological analysis of human or mouse model brain tissue may become an indicator of increased total tau and/or increased 4R/3R-tau ratio in the affected neurons. Our results also indicate that phosphorylation independent tau antibodies are more suitable when screening for neurons with nuclear indentations and excess tau by monitoring TNi incidence.

ACKNOWLEDGEMENTS

This work was supported by Centro de Investigación Biomédica en Red de Enfermedades Neurodegenerativas (CiberNed-Instituto de salud Carlos III) collaborative grant PI2013/09-2, CoEN grant (NEURO-MIR) and by grants from Spanish Ministry of Economy and Competitiveness (MINECO, SAF2012-34177 and SAF2015-65371-R), Fundación BBVA and Fundación Ramón Areces. We thank Optical and Confocal Microscopy Facilities at the Centro de Biología Molecular Severo Ochoa and the Transmission Electron Microscopy Laboratory at Universidad Autónoma de Madrid for technical support. We also thank Miriam Lucas for their excellent technical assistance and members of the Lucas' Lab for helpful advice and critical reading of the manuscript.

REFERENCES

1. Arrasate M, Perez M, Avila J. 2000. Tau dephosphorylation at tau-1 site correlates with its association to cell membrane. *Neurochemical research* 25:43-50
2. Avila J, Lucas JJ, Perez M, Hernandez F. 2004. Role of tau protein in both physiological and pathological conditions. *Physiological reviews* 84:361-84
3. Borchelt DR, Davis J, Fischer M, Lee MK, Slunt HH, et al. 1996. A vector for expressing foreign genes in the brains and hearts of transgenic mice. *Genetic analysis : biomolecular engineering* 13:159-63
4. Bots GT, Bruyn GW. 1981. Neuropathological changes of the nucleus accumbens in Huntington's chorea. *Acta neuropathologica* 55:21-2
5. Brandt R, Leger J, Lee G. 1995. Interaction of tau with the neural plasma membrane mediated by tau's amino-terminal projection domain. *The Journal of cell biology* 131:1327-40
6. Cabrera JR, Lucas JJ. 2016. MAP2 splicing is altered in Huntington's disease. *Brain pathology*
7. Cajal SR. 1909. Histologie du Système Nerveux de l'Homme et des Vertébrés. *Edition française par L. Azoulay. Consejo Superior de Investigaciones Científicas, Madrid* 1
8. Cajal SR. 1910. El núcleo de las células piramidales del cerebro humano y de algunos mamíferos. *Trab. Inst. Cajal Invest. Biol. (Madrid)* 8
9. Dawson HN, Ferreira A, Eyster MV, Ghoshal N, Binder LI, Vitek MP. 2001. Inhibition of neuronal maturation in primary hippocampal neurons from tau deficient mice. *Journal of cell science* 114:1179-87
10. Diaz-Hernandez M, Hernandez F, Martin-Aparicio E, Gomez-Ramos P, Moran MA, et al. 2003. Neuronal induction of the immunoproteasome in Huntington's disease. *J Neurosci* 23:11653-61
11. Evert BO, Wullner U, Schulz JB, Weller M, Groscurth P, et al. 1999. High level expression of expanded full-length ataxin-3 in vitro causes cell death and formation of intranuclear inclusions in neuronal cells. *Human molecular genetics* 8:1169-76
12. Fernandez-Nogales M, Cabrera JR, Santos-Galindo M, Hoozemans JJ, Ferrer I, et al. 2014. Huntington's disease is a four-repeat tauopathy with tau nuclear rods. *Nature medicine* 20:881-5
13. Frost B, Bardai FH, Feany MB. 2016. Lamin Dysfunction Mediates Neurodegeneration in Tauopathies. *Current biology : CB* 26:129-36
14. Gratuze M, Cisbani G, Cicchetti F, Planel E. 2016. Is Huntington's disease a tauopathy? *Brain : a journal of neurology* 139:1014-25
15. Graveland GA, DiFiglia M. 1985. The frequency and distribution of medium-sized neurons with indented nuclei in the primate and rodent neostriatum. *Brain research* 327:307-11
16. Hutton M, Lendon CL, Rizzu P, Baker M, Froelich S, et al. 1998. Association of missense and 5'-splice-site mutations in tau with the inherited dementia FTDP-17. *Nature* 393:702-5
17. Lamba W, Prichett W, Munoz D, Park DS, Woulfe JM. 2005. MPTP induces intranuclear rodlet formation in midbrain dopaminergic neurons. *Brain research* 1066:86-91
18. Lee VM, Goedert M, Trojanowski JQ. 2001. Neurodegenerative tauopathies. *Annual review of neuroscience* 24:1121-59
19. Mann G. 1894. Histological Changes induced in Sympathetic, Motor, and Sensory Nerve Cells by Functional Activity (Preliminary note). *Journal of anatomy and physiology* 29:100-8 1

20. Masurovsky EB, Benitez HH, Kim SU, Murray MR. 1970. Origin, development, and nature of intranuclear rodlets and associated bodies in chicken sympathetic neurons. *The Journal of cell biology* 44:172-91
21. Petry FR, Pelletier J, Bretteville A, Morin F, Calon F, et al. 2014. Specificity of anti-tau antibodies when analyzing mice models of Alzheimer's disease: problems and solutions. *PLoS one* 9:e94251
22. Roncoroni L. 1895. Su un nuovo reperto nel nucleo delle cellule nervose. *Arch Psichiati* 16
23. Roos RA, Bots GT. 1983. Nuclear membrane indentations in Huntington's chorea. *Journal of the neurological sciences* 61:37-47
24. Seress L, Ribak CE. 1992. Ultrastructural features of primate granule cell bodies show important differences from those of rats: axosomatic synapses, somatic spines and infolded nuclei. *Brain research* 569:353-7
25. Takahashi H, Egawa S, Piao YS, Hayashi S, Yamada M, et al. 2001. Neuronal nuclear alterations in dentatorubral-pallidoluysian atrophy: ultrastructural and morphometric studies of the cerebellar granule cells. *Brain research* 919:12-9
26. Vonsattel JP, Myers RH, Stevens TJ, Ferrante RJ, Bird ED, Richardson EP, Jr. 1985. Neuropathological classification of Huntington's disease. *J Neuropathol Exp Neurol* 44:559-77
27. Vuono R, Winder-Rhodes S, de Silva R, Cisbani G, Drouin-Ouellet J, et al. 2015. The role of tau in the pathological process and clinical expression of Huntington's disease. *Brain : a journal of neurology* 138:1907-18
28. Wittmann M, Queisser G, Eder A, Wiegert JS, Bengtson CP, et al. 2009. Synaptic activity induces dramatic changes in the geometry of the cell nucleus: interplay between nuclear structure, histone H3 phosphorylation, and nuclear calcium signaling. *The Journal of neuroscience : the official journal of the Society for Neuroscience* 29:14687-700
29. Woulfe J, Kertesz A, Munoz DG. 2001. Frontotemporal dementia with ubiquitinated cytoplasmic and intranuclear inclusions. *Acta neuropathologica* 102:94-102
30. Woulfe J, Munoz D. 2000. Tubulin immunoreactive neuronal intranuclear inclusions in the human brain. *Neuropathology and applied neurobiology* 26:161-71
31. Woulfe JM. 2007. Abnormalities of the nucleus and nuclear inclusions in neurodegenerative disease: a work in progress. *Neuropathology and applied neurobiology* 33:2-42
32. Woulfe JM, Hammond R, Richardson B, Sooriabalan D, Parks W, et al. 2002. Reduction of neuronal intranuclear rodlets immunoreactive for tubulin and glucocorticoid receptor in Alzheimer's disease. *Brain pathology* 12:300-7
33. Yoshiyama Y, Higuchi M, Zhang B, Huang SM, Iwata N, et al. 2007. Synapse loss and microglial activation precede tangles in a P301S tauopathy mouse model. *Neuron* 53:337-51
34. Zander C, Takahashi J, El Hachimi KH, Fujigasaki H, Albanese V, et al. 2001. Similarities between spinocerebellar ataxia type 7 (SCA7) cell models and human brain: proteins recruited in inclusions and activation of caspase-3. *Human molecular genetics* 10:2569-79

FIGURE LEGENDS**Figure 1: Transgene expression of 4R-tau in P301S results in increased total tau levels.**

A) Scheme of MoPrP-hTau.P301S transgene. The mouse prion promoter (MoPrP) drives expression of the human tau isoform 1N4R, with one N-terminal insert and four tubulin binding repeats harboring the P301S FTLD-tau mutation. **B)** Western blot detection of total tau levels with Tau5 antibody in homogenates from cortex, hippocampus and striatum of P301S mice respect to WT animals at 20 weeks of age (n=3; Student's t-test, ** $p < 0.01$, *** $p < 0.001$).

Figure 2: P301S mice show Tau Nuclear Indentations (TNIs) that highly resemble those reported in HD brains.

(A) Immunohistochemistry with HT-7 and Tau5 antibodies on sagittal sections. Images show cortex, striatum and hippocampus of P301S mice. Arrows indicate neurons with TNIs. **(B)** Cortical images of HT-7 and Tau5 immunohistochemistry on sagittal sections of WT mice. As a negative control, Tau5 immunohistochemistry on Tau KO mice was performed (lower panel). **(C)** Immunohistochemistry with phospho-specific tau antibodies on P301S mice. Tau1 (unphosphorylated tau) in 20 (left panel) and 36 (middle panel)-week old P301S mice, with detail of the different shapes that TNIs can adopt in the older mice. Squared neuron with TNI in the absence of cytoplasmic tau staining is shown magnified. AT8 (phospho-tau) immunostaining in 36-week old P301S mice (right panel). Arrows indicate neurons with TNIs. **(D)** Examples of TNIs detected with HT-7 antibody in sagittal sections of cortex and striatum of HD patients. Scale bars correspond to 5 μm .

Figure 3: Ultrastructural analysis of TNIs in P301S mice.

Immunoelectron microscopy analysis of P301S mice. Examples of cortical neurons harboring HT-7 positive rods of different shapes. Red arrows indicate the nuclear indentations with DAB precipitate signal. Scale bars correspond to 2 μm .

Figure 4: Confocal analysis confirms that TNIs fill nuclear indentations.

Immunofluorescence with HT-7 antibody and DAPI nuclear counterstaining of P301S mice neurons. Nuclear indentations and TNIs can be independently observed in cortex, hippocampus and striatum. Merge confirms that tau fills the corresponding nuclear invagination detected by DAPI. Scale bars correspond to 2.5 μm .

Figure 5: TNI appearance does not correlate with increased incidence of nuclear indentations.

(A) Confocal images showing DAPI nuclear counterstaining (upper images) and HT-7 immunofluorescence (lower images) in CA1 pyramidal neurons of WT and P301S mice. WT neurons show nuclear indentations but they are devoid of HT-7 immunofluorescence. However, the vast majority of nuclear indentations in P301S mice harbor HT-7 positive TNIs (red arrows). Blue arrows indicate nuclear indentation without TNIs. Scale bars correspond to 2.5 μm . **(B)** Quantification of the incidence of TNIs detected by HT-7 immunofluorescence (left histogram, n=3) and nuclear indentations detected by DAPI counterstaining (right histogram, n=5 for WT, n=7 for P301S) in CA1 hippocampal neurons.

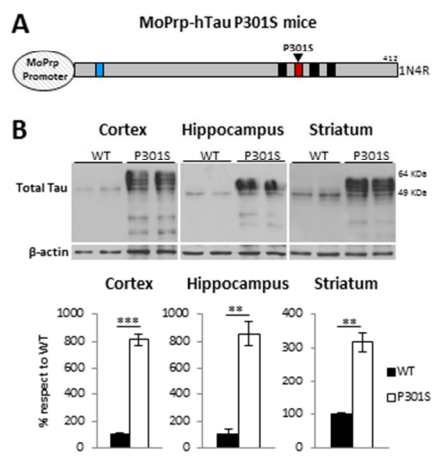


Figure 1

190x254mm (96 x 96 DPI)

AC

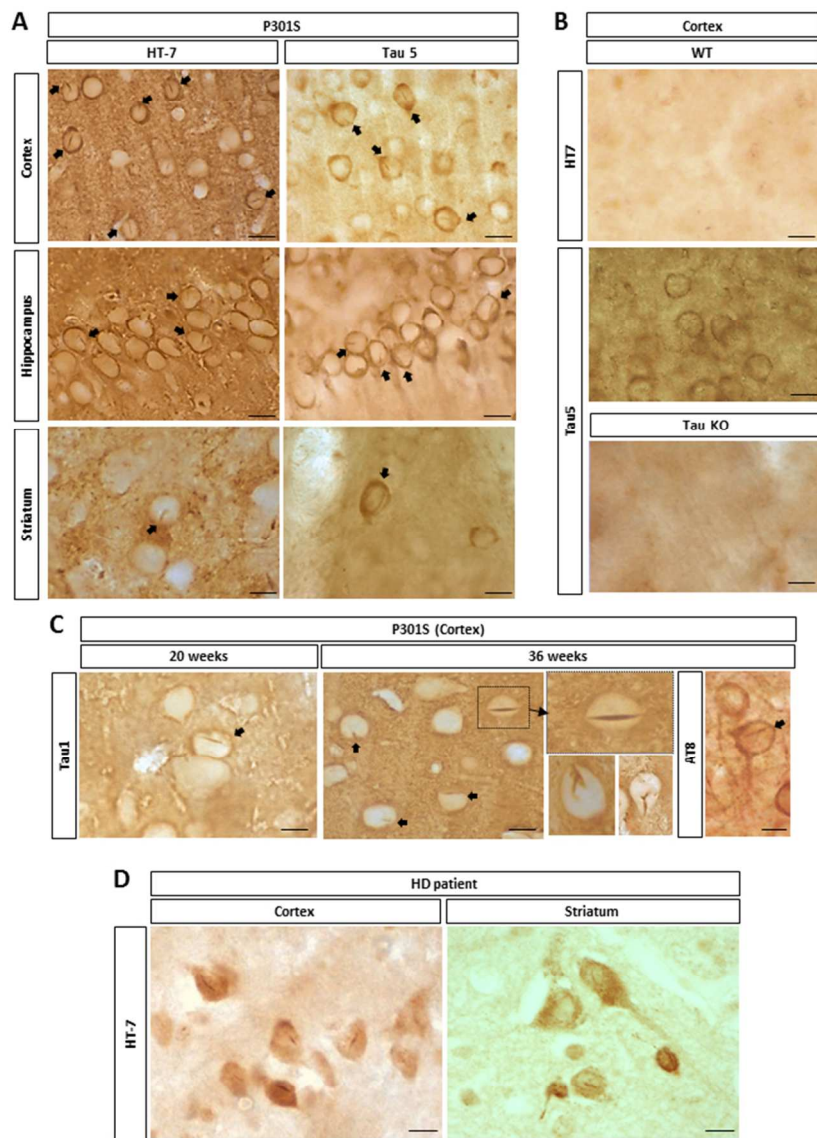


Figure 2

190x254mm (96 x 96 DPI)

AC

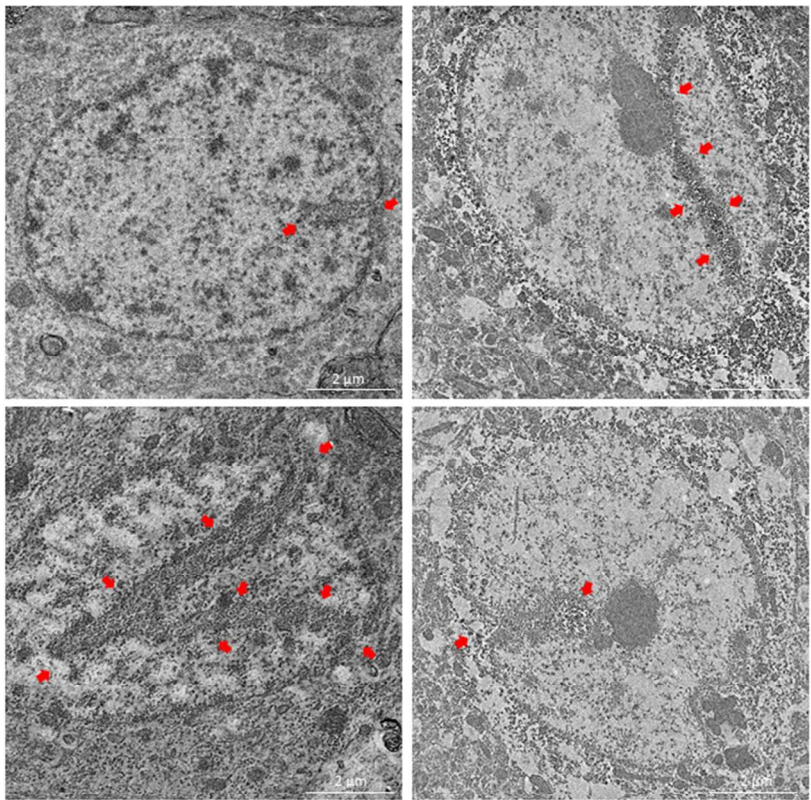


Figure 3

190x254mm (96 x 96 DPI)

AC

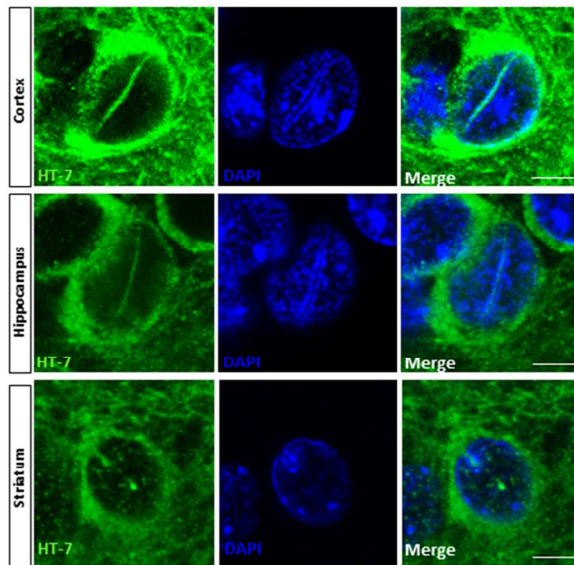


Figure 4

190x254mm (96 x 96 DPI)

AC

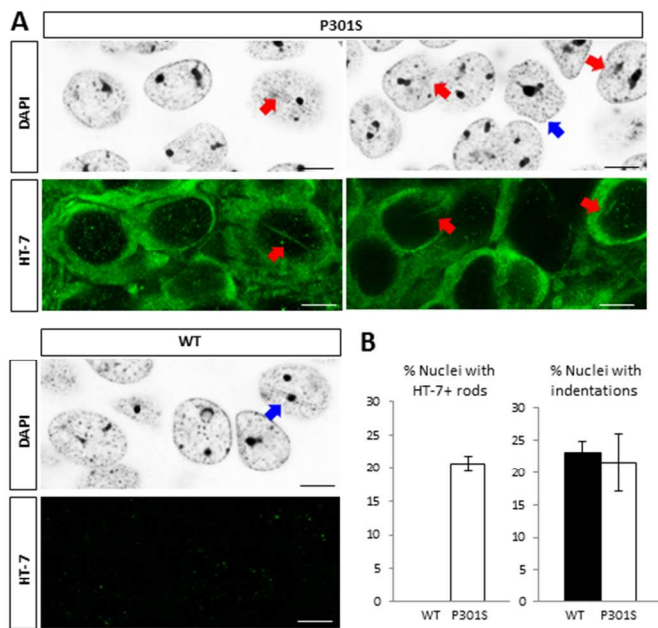


Figure 5

190x254mm (96 x 96 DPI)

AC